

Deeper Insight into the Six-Step Domino Reaction of Aldehydes with Malononitrile and Evaluation of Antiviral and Antimalarial Activities of the Obtained Bicyclic Products

Christina M. Bock,^[a] Gangajji Parameshwarappa,^[a] Simon Bönisch,^[b] Walter Bauer,^[a] Corina Hutterer,^[c] Maria Leidenberger,^[d] Oliver Friedrich,^[d] Manfred Marschall,^[c] Barbara Kappes,^[d] Andreas Görling,^[b] and Svetlana B. Tsogoeva*^[a]

The straightforward and efficient synthesis of complex aza- and carbobicyclic compounds, which are of importance for medicinal chemistry, is a challenge for modern chemical methodology. An unprecedented metal-free six-step domino reaction of aldehydes with malononitrile was presented in our previous study to provide, in a single operation, these bicyclic nitrogen-containing molecules. Presented here is a deeper investigation of this atom-economical domino process by extending the scope of aldehydes, performing post-modifications of domino products, applying bifunctional organocatalysts and comprehensive NMR studies of selected domino products. The thermodynamic aspects of the overall reaction are also demon-

strated using DFT methods in conjunction with a semi-empirical treatment of van der Waals interactions. Furthermore, biological studies of seven highly functionalized and artemisinin-containing domino products against human cytomegalovirus (HCMV) and *Plasmodium falciparum* 3D7 are presented. Remarkably, in vitro tests against HCMV revealed five domino products to be highly active compounds (EC₅₀ 0.071–1.8 μM), outperforming the clinical reference drug ganciclovir (EC₅₀ 2.6 μM). Against *P. falciparum* 3D7, three of the investigated artemisinin-derived domino products (EC₅₀ 0.72–1.8 nM) were more potent than the clinical drug chloroquine (EC₅₀ 9.1 nM).

1. Introduction

The domino process is a powerful tool to economically and sustainably build complex molecular architectures.^[1] The number of work-up and purification steps is drastically reduced, therefore, the procedure is less time-consuming and produces less waste compared to traditional stop-and-go synthesis. Typical steps involved in known domino processes are different C–C bond formation reactions, for example, Michael, aldol or Knoevenagel reactions,^[2] which in combination can lead to highly substituted carbocyclic compounds,^[3] spirocyclic structures^[4] or diverse heterocycles.^[5]

Nitrogen-containing bicyclic systems, among them isoquinuclidine (2-azabicyclo[2.2.2]octane) and carbobicycles with an

exocyclic imine group (bicyclo[2.2.2]octan-2-imine) are found as subunits in numerous natural products and bioactive compounds,^[6] but are not easy to access using common synthetic methods. Only a few organocatalytic methods for generation of these ring systems have been reported.^[7] The known metal-free and metal-catalyzed methods for the synthesis of azabicycles and carbobicycles often use reagents that are not commercially available and require laborious precursor synthesis and isolation and/or purification of intermediate products in most cases.^[7,8] Notably, there are only a few examples in the literature for the formation of isoquinuclidines starting from readily available alkyldenemalononitriles under metal-cata-

[a] C. M. Bock, Dr. G. Parameshwarappa, Prof. Dr. W. Bauer, Prof. Dr. S. B. Tsogoeva
Institute of Organic Chemistry I and
Interdisciplinary Center for Molecular Materials
Friedrich-Alexander-University Erlangen-Nürnberg
Henkestrasse 42, 91054 Erlangen (Germany)
E-mail: svetlana.tsogoeva@fau.de

[b] S. Bönisch, Prof. Dr. A. Görling
Chair of Theoretical Chemistry and
Interdisciplinary Center for Molecular Materials
Friedrich-Alexander-Universität Erlangen-Nürnberg
Egerlandstraße 3, 91058 Erlangen (Germany)

[c] Dr. C. Hutterer, Prof. Dr. M. Marschall
Institute for Clinical and Molecular Virology
Friedrich-Alexander-Universität Erlangen-Nürnberg
Schlossgarten 4, 91054 Erlangen (Germany)

[d] M. Leidenberger, Prof. Dr. O. Friedrich, Prof. Dr. B. Kappes
Institute of Medical Biotechnology
Friedrich-Alexander-Universität Erlangen-Nürnberg
Paul-Gordan-Straße 3, 91052 Erlangen (Germany)

Supporting Information and the ORCID identification number(s) for the author(s) of this article can be found under:
<https://doi.org/10.1002/open.201700005>.

© 2017 The Authors. Published by Wiley-VCH Verlag GmbH & Co. KGaA. This is an open access article under the terms of the Creative Commons Attribution-NonCommercial-NoDerivs License, which permits use and distribution in any medium, provided the original work is properly cited, the use is non-commercial and no modifications or adaptations are made.

lyzed conditions.^[9] Recently, we reported the discovery of a two-component multi-step domino reaction under metal-free conditions providing both carbobicyclic compounds with exocyclic imine groups and azabicycles (isoquinuclidines).^[10] In this context, we demonstrated the generation of intricate molecular architectures from simple aldehydes and malononitrile in a single operation by a six-step domino reaction. Imidazole was found to be the most suitable achiral catalyst for this atom-economical reaction and was successfully applied to study the reaction scope using substituted 2-phenylacetaldehydes.^[10] Propanal as a representative aliphatic starting material showed that this reaction is not limited to phenylacetaldehyde derivatives. This study was complemented with mechanistic investigations using mass spectrometry (MS) techniques and DFT calculations taking into account van der Waals interactions.

Developing such new and straightforward syntheses for these classes of compounds is of great interest due to their enormous potential as pharmaceuticals, demonstrated by a number of studies on their biological activities.^[6,11] Inspired by naturally occurring alkaloids, compounds such as ibogaine analogue **A** have recently been synthesized and biologically evaluated (Figure 1).^[6d] Isoquinuclidine analogue **A** has been

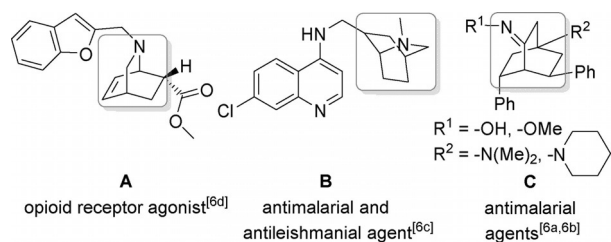


Figure 1. Selected examples of bioactive azabicyclic (**A** and **B**) and carbobicyclic compounds with exocyclic imine groups (**C**).

characterized as an opioid receptor agonist with potential analgesic properties. Similar to its chloroquine-type parent compound, isoquinuclidine derivative **B** (Figure 1) possesses antimalarial and antileishmanial activities.^[6c] Carbobicyclic compounds with an exocyclic imine function (**C**, Figure 1) appear to have comparable antimalarial activities.^[6a,b]

Motivated by these promising examples, we investigated the potential antimalarial and antiviral activities of our domino products. Herein, we present the results of these biological studies in addition to our extended scope of substrates and bifunctional catalysts for the six-step domino reaction, and an extensive NMR spectroscopic analysis of a selected domino product.

2. Results and Discussion

2.1. Extended Substrate and Catalyst Scope for the Domino Reaction

In our previous study, we mainly focused on substituted phenylacetaldehydes as substrates.^[10] With 11 different examples,

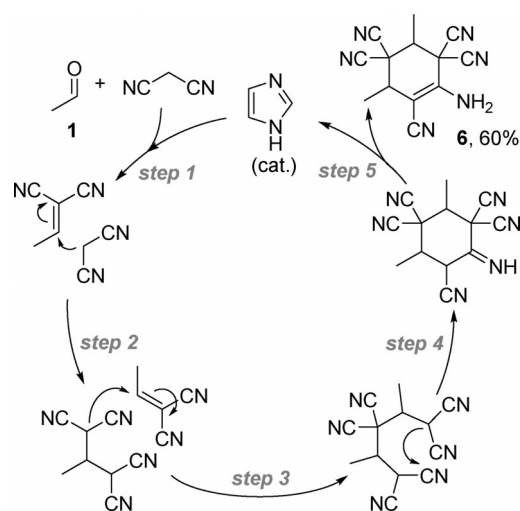
we demonstrated the broad substrate tolerance of this multi-step domino reaction; propanal was the only aliphatic aldehyde tested. Starting from those results with propanal, in this study we performed a series of experiments with homologous aliphatic aldehydes (Table 1).

Table 1. Extended substrate scope of the imidazole-catalyzed multi-step domino reaction.

Entry	Aldehyde	Products	Yield [%] ^[c]	d.r. a (anti/syn) ^[d]	Ratio a/b ^[d]
1 ^[a]		1 a, 1 b	–	–	–
2 ^[b]		2 a, 2 b	25	38:62	11:1
3		3 a, 3 b	23	40:60	2:1
4		4 a, 4 b	13	47:53	1:1
5		5 a, 5 b	25	> 99:1	1:3

[a] “–”: 0% yield. [b] The reaction has been previously reported.^[10] [c] Sum of yields of isolated products **a** and **b**. [d] Determined by ¹H NMR spectroscopy (see the Supporting Information).

Use of the shorter homologue acetaldehyde (**1**) did not lead to the expected domino products **1 a** and **1 b** (Table 1, entry 1). Instead, the cyclohexene derivative **6**, bearing five nitrile groups, was obtained in 60% yield (Scheme 1). Notably, similar findings had been reported earlier in a study of base-catalyzed condensation reactions with different alkylidenemalononitriles.^[12] How can this reaction outcome be explained? Obviously, there is a change in the sequence of the reaction steps in the catalytic cycle. The first step is a Knoevenagel reaction of acetaldehyde and malononitrile (Scheme 1, step 1), similar to the first step in the reaction mechanism previously pro-



Scheme 1. Imidazole-catalyzed five-step domino reaction of acetaldehyde (**1**) with malononitrile.

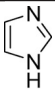
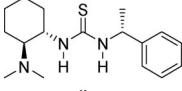
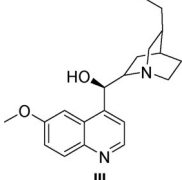
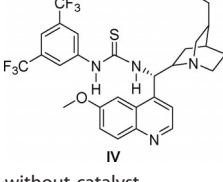
posed for the formation of bicyclic domino products.^[10] Next follows a 1,4-conjugate addition of malononitrile to the Knoevenagel product (Michael acceptor; Scheme 1, step 2).

The reaction with another Knoevenagel product molecule leads, through subsequent three steps (Scheme 1, steps 3–5), to the generation of cyclohexene **6**. By contrast, the azabicyclo **7a** and carbobicyclo **7b** were likely formed when phenylacetaldehyde was used instead of acetaldehyde (Table 2, entry 1). This is because a dimerization reaction (vinylogous Michael addition) of the Knoevenagel product (generated from phenylacetaldehyde)^[10] occurs before another molecule of malononitrile can attack it. These differences between the reaction mechanisms indicate the complexity of this domino reaction and demonstrate how drastically reaction outcome, and therefore the product, can change, even if there are only small differences in aldehyde structure.

The experiments with butyraldehyde (**3**) and valeraldehyde (**4**) showed that with longer chain length of the aliphatic aldehyde, yield and selectivity of the reaction decrease (Table 1, entries 3 and 4). For **3**, the yield of 23% and the d.r. (**3a**, *anti/syn*)

of 40:60 were similar to the results obtained with propanal (**2**). However, there was a loss of selectivity in the formation of the two constitutional isomers **3a** and **3b** (their ratio was 2:1). With a low yield of 13% and almost no selectivity towards any isomer, use of **4** as the substrate led to the worst results. As a final example of the substrate scope, 3-phenylpropanal (**5**) was chosen. This substrate also contains a phenyl group, like the originally used phenylacetaldehyde (**7**), although there is no enhanced reactivity, because the benzylic position is not α to the carbonyl group. Compared to the reaction with **7** (Table 2, entry 1), the yield for the reaction with **5** was lower at 25%, whereas the high diastereoselectivity was preserved, and only the *anti* isomer of **5a** was formed (Table 1, entry 5). Remarkably, this was the only example for which the isoquinuclidine was formed in a lower amount than the iminocarbocyclic compound (**5a/5b** = 1:3). The lower yield could be explained by the less reactive aldehyde, but the steric demand of the phenyl ring was apparently still sufficient to prevent the formation of a *syn-5a* isomer.

Table 2. Catalyst and solvent screening for the reaction of phenylacetaldehyde (**7**) with malononitrile.

Entry	Catalyst	Solvent	Time [h]	Yield [%] ^[a]	Ratio 7a/7b ^[b,c]	d.r. 7a (<i>anti/syn</i>)	d.r. 7b
1		toluene	48	52	4:1	> 99:1	50:50
2		toluene	24	52	1:11	> 99:1	33:67
3		toluene	26	70	1:22	> 99:1	50:50
4		toluene	25	83	1:25	> 99:1	25:75 ^[d]
5 ^[e]	without catalyst	toluene	22	–	–	–	–
6	IV	CH ₂ Cl ₂	24	79	1:19	> 99:1	33:67
7	IV	hexane	72	53	2:1	> 99:1	50:50
8	IV	C ₆ F ₆	24	69	1:2	> 99:1	33:67
9	IV	MeOH	23	50	1:7	> 99:1	50:50

[a] Sum of yields of isolated products **7a** and **7b**. [b] **7a/7b** ratio determined by HPLC. [c] HPLC conditions for the separation of enantiomers and determination of *ee* values of obtained products were not found. [d] Enantioselectivities of the major product **7b** (48% and 47% *ee* for two diastereomers, respectively) were determined by ¹H NMR spectroscopy in presence of the chiral shift reagent Eu(hfc)₃. [e] “–”: 0% yield.

Although the focus of this work was not the development of an enantioselective version of this new reaction, nonetheless we probed the potential of converting the formation reaction of **7a** and **7b** into an enantioselective synthesis route. Therefore, we also used tertiary-amine-based bifunctional chiral organocatalysts **II–IV** (Table 2). However, we did not find HPLC conditions for determination of the *ee* values of the obtained products and hence we limited our studies to determination of yields, **7a/7b** ratios and diastereoselectivities for **7a** and **7b**. Nonetheless, to measure the enantioselectivity for products obtained with the selected bifunctional chiral catalyst **IV** (providing the best reaction outcome), we used ^1H NMR spectroscopy in the presence of chiral shift reagent $\text{Eu}(\text{hfc})_3$ [$\text{hfc} = 3$ -(heptafluoropropylhydroxymethylene)-*D*-camphorate].

The carbobicyclic **7b** dominates with chiral catalysts **II–IV** in toluene as a solvent (the **7a/7b** ratio ranges from 1:11 to 1:25, see Table 2). This constitutes strong evidence for kinetic control in the formation of **7b**, also implied by the observed enantiomeric excess of **7b** (*ee* values of 48% and 47% for the two corresponding diastereomers of **7b**, Table 2). Strikingly, the overall yield (after all six steps) could be increased to a maximum of 83% using catalyst **IV** (Table 2, entry 4). Interestingly, in all investigated solvents (toluene, CH_2Cl_2 , hexane, C_6H_6 and MeOH) the constitutional isomer **7a** was formed as a single diastereomer (*d.r.* > 99:1). However, although solvents have a strong impact on yields and chemoselectivities, a clear trend is not apparent (Table 2, entries 6–9).

In summary, the chemoselectivity and the reaction yield of this domino process in toluene is highly dependent on the choice of substrate and catalyst. Therefore, the control over the chemoselectivity might be possible through the use of a particular aldehyde or organocatalyst (see Tables 1 and 2).

2.2. DFT Studies on the Thermodynamics of the Overall Reaction

In our recent study, we considered the thermodynamic and kinetic aspects of the chemodivergent step.^[10] From these calculations, one could deduce that the Michael reaction (**D**→**H**, Figure 2) is faster, whereas the intermolecular addition reaction (**D**→**E**, Figure 2) is thermodynamically favored. The reaction barriers were somewhat moderate and the initial reaction from **D** to both **E** and **H** is endergonic. Therefore, we concluded that the subsequent steps might also play a role. To further shed light on this reaction, we studied the thermodynamics of the subsequent steps of both reaction pathways by calculating the intermediates resulting in **7a**, that is, **F** and **G** (the imine tautomer of **7a**), as well as the intermediates resulting in **7b**, that is, **I** and the more stable enamine tautomer **J** (Figure 2). Computational details can be found in the Supporting Information.

The product of the initial ring closure (**E**→**F** or **H**→**I**) is energetically lower by $17.7 \text{ kcal mol}^{-1}$ for the pathway to **7a**. After the tautomerization to the more stable enamine **J**, this effect is only partly compensated and the intermediate **F** of the pathway to **7a** is, therefore, favored thermodynamically at this stage by $5.4 \text{ kcal mol}^{-1}$ over intermediate **J**. The bicyclic **G** of the pathway to **7a** is thermodynamically slightly favored by $0.6 \text{ kcal mol}^{-1}$ over product **7b**, whereas the reaction from **F** to **G** is less exergonic with a reaction free energy of $-2.2 \text{ kcal mol}^{-1}$ compared to $-7.1 \text{ kcal mol}^{-1}$ for the formation of **7b** from **J**. Unlike **7b**, the imine (**G**) can undergo tautomerization to the enamine **7a**, which is $11.7 \text{ kcal mol}^{-1}$ more stable than **7b**. Without dispersion interactions the free energies of the first intermediates **E** and **H** would be considerably higher (Figure 2), whereas the subsequent reaction steps for both pathways exhibit similar reaction free energies to those if dispersion is taken into account. The raising of the free energy of

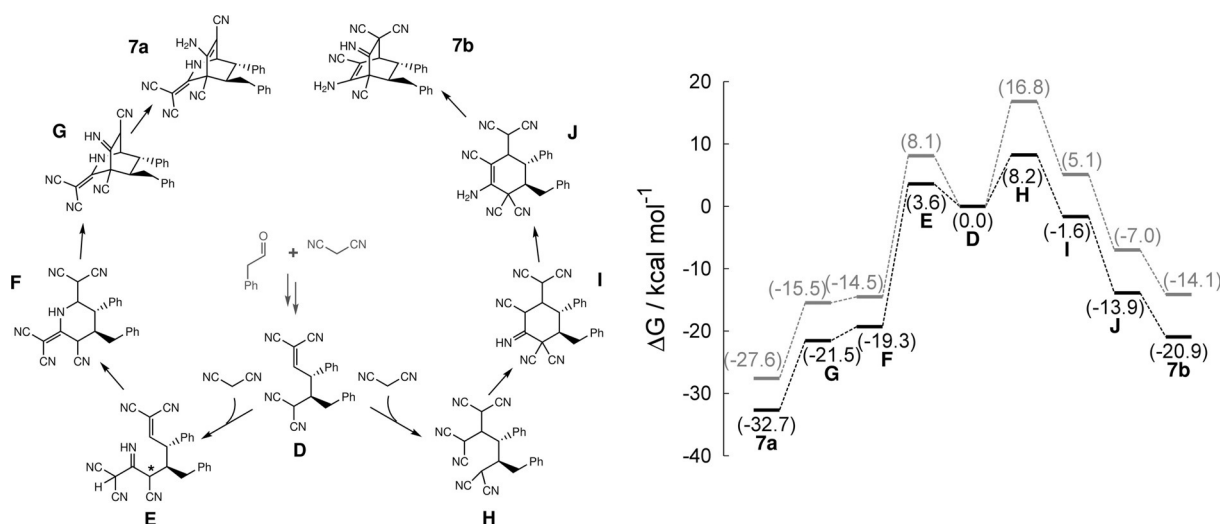


Figure 2. Left: Modified version of the mechanism reported in our previous publication.^[10] Right: Free energies [kcal mol^{-1}] of the most stable conformers of the intermediates leading to **7a** and **7b**, respectively, relative to the reactants (**D** plus malononitrile), with (black) and without (gray) dispersion interactions taken into account in the geometry optimization and calculation of free energies.

the first intermediate indicated previously^[10] is stronger for **H** compared to **E**, which means the pathway leading to product **7b** benefits more from dispersion interactions.

Overall it seems that the path with the initial addition reaction (**D**→**E**) is thermodynamically favored and its product **7a** is favored owing to the tautomerization to the enamine.

2.3. NMR Investigations of a Selected Domino Product

Selected findings of our extensive NMR spectroscopic study of isoquinulidine *syn-2a* was discussed in our previous publication^[10] on this metal-free multi-step domino reaction. More details gained from the use of methods such as HMQC, HMBC, correlation via long-range coupling (COLOC), COSY, NOESY, and ¹H–¹³C heteronuclear NOESY (HOESY) are presented in this section. For convenience, we refer to the atom numbering shown in Figure 3.

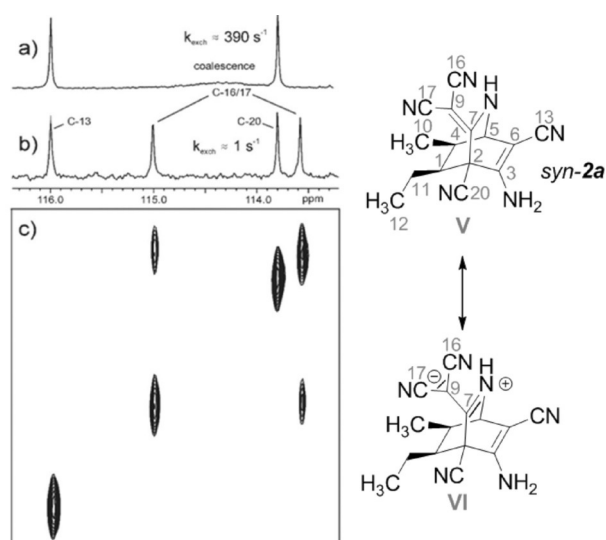


Figure 3. Left: Zoomed ¹³C NMR spectra (125 MHz) of *syn-2a* at +25 °C, showing the four CN signals. Numbering is as suggested by the NMRPredict software.^[13] a) Spectrum in [D₆]DMSO; note the coalescence of the C-16 and C-17 signals; b) spectrum in [D₆]DMSO/CD₃CN (1:2); note the slow exchange rates of C-16 and C-17; c) the EXSY spectrum; the cross peaks indicate the chemical exchange of positions 16 and 17; mixing time 2.5 s, measuring time 7.7 h. Right: Two mesomeric structures of *syn-2a*. In pure [D₆]DMSO, structure **VI** is more preferred over structure **V** than in a mixture of [D₆]DMSO/CD₃CN (1:2).

As is often the case, the assignment of the quaternary carbon signals in the ¹³C NMR spectrum of *syn-2a* was not straightforward. In particular, the nitrile carbons presented a challenge. However, in the COLOC spectrum (not shown) there is an intense cross peak between the H-5 signal and the carbon signal at 116.00 ppm, originating from ³J coupling. This carbon signal can therefore be assigned to C-13. Along with the dynamics findings (see below), the other CN signals could also be assigned.

The CSEARCH/NMRPredict software package^[13] is a powerful tool for estimating ¹³C NMR chemical shifts in a given structure. Table 3 shows a comparison of predicted and experimental

C atom	NMRPredict [ppm]	Experiment [ppm]
1	44.5	46.4
2	54.3	52.8
3	148.1	154.7
4	41.1	37.1
5	53.8	56.8
6	79.1	75.7
7	152.7	160.7
9	58.2	48.8
10	16.5	14.3
11	20.6	21.4
12	13.3	13.8
13	112.0	116.0
16	115.3	115.0 ^[a]
17	115.3	113.6 ^[a]
20	118.5	113.8

[a] Assignment may be reversed.

¹³C NMR shifts; a good coincidence is evident. A discrepancy was found for the chemical shift sequence of C-13 and C-20. Here, our COLOC findings clearly indicate the experimental values to be correct. Strong deviations were also found for the olefinic carbons C-7 and C-9. These deviations might be explained by the mesomeric effects described below in reference to the molecular dynamics.

Interesting observations were made on the intramolecular dynamics in *syn-2a*. Our initial ¹³C and ¹⁵N spectra were recorded in [D₆]DMSO. To our surprise, only two ¹³C signals and two ¹⁵N signals for the CN groups were observed under these conditions. A closer inspection of these spectra showed the two missing signals to be coalescing. However, if a mixture of [D₆]DMSO and CD₃CN (1:2) were used, all four expected CN signals were resolved in the ¹³C and ¹⁵N spectra. Under these conditions, the chemical exchange of the CN groups involving C-16 and C-17 is considerably slower. Figure 3 shows the ¹³C region of the CN signals. Figure 3a represents a spectrum recorded in [D₆]DMSO. Note that there is coalescence of C-16 and C-17. All of the expected four signals were observed in the spectrum recorded in the mixture of [D₆]DMSO and CD₃CN (Figure 3b). Under these conditions, there is slow exchange of the C-16 and C-17 positions.

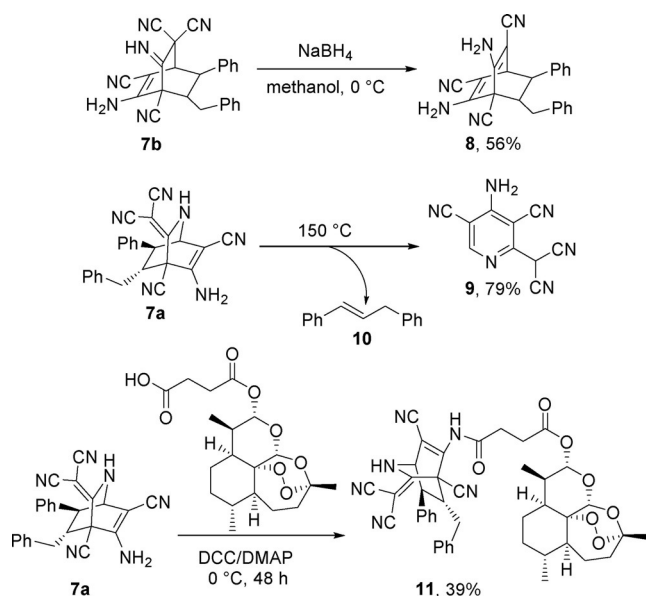
A ¹³C–¹³C exchange spectroscopy (EXSY) spectrum (Figure 3c) corroborates these findings: the cross peaks found clearly indicate mutual exchange of these two CN positions. From the cross peak intensities we conclude the exchange rate to be in the order of approximately 1 s⁻¹. In contrast, by using the difference in chemical shifts of C-16 and C-17 under slow-exchange conditions, the Gutowsky–Holm equation ($k_{\text{exch}} = 2.22 \Delta\nu$) leads to an estimated exchange rate of approximately 390 s⁻¹ in pure [D₆]DMSO.

We interpret these dramatic differences in exchange rates as a consequence of different hydrogen bonding between NH groups and the solvent. In classical terms, the structure of *syn-2a* can be formulated as two mesomeric forms (Figure 3). In structure **V**, there is a “true” double bond between C-7 and C-9. By contrast, the zwitterionic structure **VI** shows a formal

single bond between these two carbon atoms, with a much lower barrier of exchange activation energy. Structure **VI** is more preferred over structure **V** in pure $[D_6]DMSO$ as compared to the solvent mixture. Tentatively, we interpret this observation as follows: it is well known that proton exchange is considerably slower in pure DMSO.^[14] In an NH group, the proton “resides/sticks” at its nitrogen atom. Hence, the nitrogen is more prone to carry a positive charge as in structure **VI**, leading to a higher single bond character of C-7–C-9. If the solvent ($[D_6]DMSO$) is diluted with CD_3CN , the NH proton exchange becomes more facile and rapid. The NH proton is considered more “loose” under these conditions. Thus, structure **V** with its true C-7=C-9 double bond becomes more abundant, thus the C-16–C-17 exchange rate is slower.

2.4. Post-Modification of the Domino Products

As a further part of our investigations we were interested in chemical post-modifications of our domino products to potentially introduce these types of compounds to a wider field for future applications. Three transformations that were performed are depicted in Scheme 2.



Scheme 2. Post-modifications of domino products **7a** and **7b**.

Iminocarbocycle **7b** was transformed in the presence of sodium borohydride to bicyclo[2.2.2]-octa-diene **8** with the elimination of one cyano group. As it was not possible to obtain an X-ray crystal structure of **7b**, the formation of **8** provides further evidence for the presence of the imine function in the parent compound **7b**. The two most downfield-shifted signals in the ^{13}C NMR spectrum of **8** at around 156 ppm fit well the theoretical value of the two carbons adjacent to the NH_2 groups. Under the reducing conditions, this second amino group can only originate from the imine function. Also worth

mentioning here is the exceptional stability of this imine function. Compound **7b**, for instance, remained completely unconverted upon treatment with mild reducing agents such as trichlorosilane.

For isoquinuclidine **7a**, the thermal degradation to highly substituted pyridine derivatives^[9b] was tested. The reaction was conducted under neat conditions at a temperature of $150\text{ }^\circ\text{C}$. The formation of the elimination product **10** was confirmed by comparison with literature data. Surprisingly, pyridine derivative **9** showed only two signals in the 1H NMR spectrum and not three, as one might expect. It is likely that an intermolecular deprotonation of the dicyanomethyl group CH proton through the nitrogen atom of the pyridine core occurred; only a zwitterionic structure, which is detected in solution can explain the missing NMR signal.

The synthesis of hybrid compound **11**, consisting of isoquinuclidine and artemisic acid subunits, is the final example of post-modification presented herein. The reaction to form the amide bond was accomplished in the presence of *N,N'*-dicyclohexylcarbodiimide (DCC) and 4-dimethylaminopyridine (DMAP). Comparable amide-bond-forming reagents such as 1-ethyl-3-(3-dimethylaminopropyl)carbodiimide and hydroxybenzotriazole were not able to successfully activate the substrates in this case. Product **11** was obtained in 39% yield starting from isoquinuclidine **7a** and artemisic acid under DCC/DMAP activation after stirring at $0\text{ }^\circ\text{C}$ for 48 h.

2.5. Antiviral and Antimalarial Activities of Highly Functionalized Domino Products

Currently, there is a requirement for novel antiviral and antimalarial compounds with high efficacy and low unintended side effects. Therefore, the development of such therapeutics has concentrated on discovering drug candidates that operate selectively and effectively against viruses and malaria. A promising and fundamentally novel approach to obtain new and efficacious compounds with improved pharmacological properties is the hybridization of bioactive natural products, in which two or more natural product fragments are covalently linked with each other to form new hybrid molecules.^[15] These synthetic hybrids containing partial structures of natural compounds are in most cases more active than their parent compounds.^[16] Encouraged by our previous results and experience with artemisinin-based hybrids^[17] we demonstrate here the high potential of our domino-product–artemisinin hybrid molecules **11**, **12a/b** and **13a/b** (Figure 4) as antiviral and antimalarial agents. For comparison, we also present the activities of parent domino products **7a** and **7b** (not containing artemisinin moieties) against human cytomegalovirus (HCMV) and *Plasmodium falciparum* 3D7.

2.5.1. Antiviral Activity

The anti-HCMV activity of the new domino products and their artemisinin-based hybrids was evaluated by the use of an established GFP-reporter-based replication assay of HCMV (recombinant strain AD169-GFP) in primary human foreskin fibro-

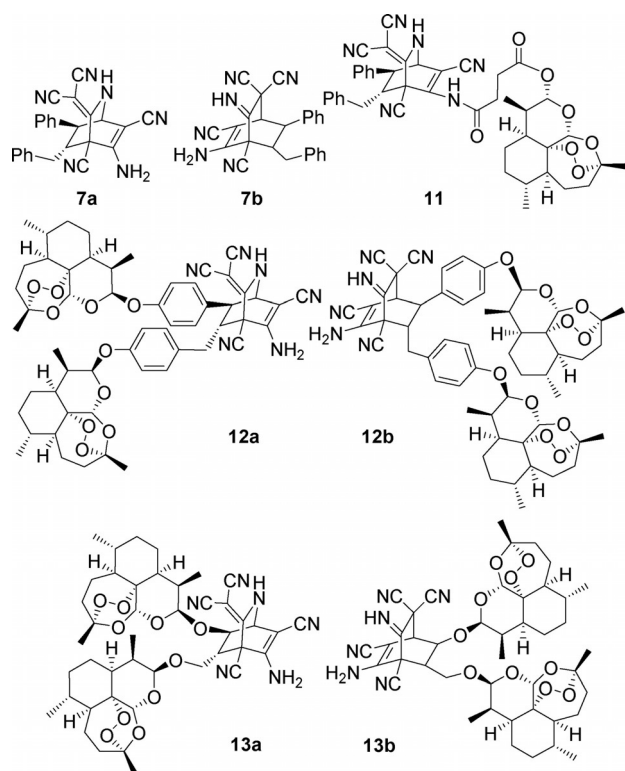


Figure 4. The domino products evaluated against human cytomegalovirus (HCMV) and the parasite *P. falciparum* 3D7 in this work.

blasts (HFFs).^[18] Ganciclovir, an approved drug mostly applied in conventional anti-HCMV therapy, and artemisinin, representing the parent compound of our novel hybrid products, were used as reference compounds. Whereas ganciclovir displayed an EC_{50} value of inhibition of HCMV replication in the low micromolar range (EC_{50} $2.6 \pm 0.5 \mu\text{M}$), artemisinin exerted no measurable inhibitory effect within the range of analysis ($EC_{50} > 10 \mu\text{M}$). Remarkably, five (**7b**, **12a/b**, **13a/b**, see Figure 4) out of seven tested domino products showed higher antiviral activity than the reference compounds (Table 4). Only isoquinu-

Table 4. EC_{50} values of anti-HCMV activity (AD169-GFP) displayed in virus-infected HFFs: ganciclovir, artemisinin and compounds **7a**, **7b**, **11**, **12a**, **12b**, **13a** and **13b**.

Compound	Molecular weight [Da]	EC_{50} [μM] ^[a]
Ganciclovir ^[b]	255.23	2.6 ± 0.50
Artemisinin ^[b]	282.34	> 10
7a	402.46	> 10
7b	402.46	1.84 ± 0.15
11	768.87	> 10
12a ^[c]	967.13	0.07 ± 0.00
12b ^[c]	967.13	0.26 ± 0.01
13a	814.94	0.21 ± 0.00
13b	814.94	0.22 ± 0.00

[a] Mean values \pm SD were calculated from replicates, $n=4$ (all data sets were confirmed by performing two independent experiments). [b] EC_{50} values have been previously reported.^[19] [c] EC_{50} values have been previously reported.^[10]

clidine **7a** and the artesunic acid-derived hybrid **11** showed no measurable activity (EC_{50} values $> 10 \mu\text{M}$). An outstanding result was obtained with the isoquinuclidine–artemisinin hybrid **12a**, as characterized by the HCMV-specific EC_{50} value of $0.071 \mu\text{M}$, which represents a 37-fold increase in in vitro efficacy over the established therapeutic ganciclovir. Other active domino products (**7b**, **12b**, **13a** and **13b**) were effective, with a range of EC_{50} values between 0.21 and $1.8 \mu\text{M}$, thus showing similar or higher activity than ganciclovir. This study shows the eminent potential of the hybrid concept, as active hybrids **12a**, **12b**, **13a** and **13b** featured strong antiviral properties against HCMV, outperforming the parent compounds (artemisinin, **7a** and **7b**) and ganciclovir.

2.5.2. Antimalarial Activity

The antimalarial activities of the domino products **7a**, **7b**, **11**, **12a**, **12b**, **13a** and **13b** (see Figure 4) were assessed by in vitro cytotoxicity studies against the *P. falciparum* 3D7 strain using chloroquine and dihydroartemisin (DHA) as reference compounds (Table 5). Both control substances displayed EC_{50} values in the low-nanomolar range (9.1 and 2.3 nM, respective-

Table 5. EC_{50} values for chloroquine, dihydroartemisin and compounds **7a**, **7b**, **11**, **12a**, **12b**, **13a** and **13b** tested against the parasite *P. falciparum* 3D7.

Compound	Molecular weight [Da]	EC_{50} [nM] ^[a]
Chloroquine	319.87	9.1 ± 1.0
Dihydroartemisin	284.35	2.3 ± 0.4
7a	402.46	$> 1 \mu\text{M}$
7b	402.46	$> 1 \mu\text{M}$
11	768.87	1.8 ± 0.6
12a	967.13	17.0 ± 3.0
12b	967.13	63.0 ± 25.0
13a	814.94	1.5 ± 0.3
13b	814.94	0.72 ± 0.2

[a] Mean values \pm SD were calculated from at least three independent biological replicates ($n \geq 3$) and each of these data sets consisted of three separate measurements (see the Experimental Section).

ly). Domino products **7a** and **7b**, prepared from phenylacetaldehyde, possessed only a minor inhibitory activity in the lower micromolar range against the 3D7 strain. With EC_{50} values of 17 and 63 nM, the hybrid domino products **12a** and **12b** exhibited a higher antimalarial activity in the mid-nanomolar range. However, these EC_{50} values were significantly higher than that of their parent compound DHA. In contrast to these findings, artesunic-acid–isoquinuclidine hybrid **11** nicely demonstrated a cooperative and synergistic effect of the 1,2,4-trioxane and isoquinuclidine moieties. With an EC_{50} value of 1.8 nM, it is nearly five times more active than the parent compound artesunic acid ($EC_{50}=8.9$ nM) and comparable in activity to DHA ($EC_{50}=2.3$ nM), although the parent isoquinuclidine **7a** was inactive.

The best result was that achieved with hybrid domino product **13b**, which outperformed both reference compounds, with a remarkable EC_{50} value of 0.72 nM, followed by its constitutional isomer **13a** with a value of 1.5 nM.

3. Conclusions

In summary, we present a more thorough investigation of the recently introduced imidazole-catalyzed six-step domino reaction, providing a direct and convenient route to bioactive azabicyclic and carbobicyclic compounds.^[10] We have demonstrated the extension of the substrate scope towards aliphatic aldehydes with longer chain lengths and found a reversed chemoselectivity of this reaction in the case of 3-phenylpropanal (**5**). As well as imidazole, different bifunctional organocatalysts have been investigated for the reaction of phenylacetaldehyde (**7**) with malononitrile. The most active catalyst in this screening was the dihydroquinine-derived thiourea **IV**, use of which led to the domino products **7a** and **7b** in a high overall yield of 83% and high chemoselectivity towards the carbobicycle **7b** (**7a/7b**=1:25). It is apparent that the chemoselectivity of this domino process is strongly dependent on the choice of substrate and the catalyst and, therefore, the control over the chemoselectivity might be possible through the use of a particular aldehyde or organocatalyst.

To further investigate the chemodivergent domino process, and to understand the influence of dispersion interactions, we studied the thermodynamics of the steps of both reaction pathways (leading to **7a** and **7b**, correspondingly) by DFT calculations of the intermediates both without and with dispersion interactions. We found that the pathway leading to product **7b** is more favored with dispersion interactions. Furthermore, a range of NMR techniques (HMQC, HMBC, COLOC, COSY, NOESY, and 1H - ^{13}C HOESY) was used for determining the structure of the isoquinuclidine *syn*-**2a**, formed from propanal. A strongly solvent-dependent exchange of the two nitrile groups adjacent to the exocyclic double bond was detected.

The study was completed by post-modifications of domino products **7a** and **7b** and the investigation of their antiviral and antimalarial properties, as well as selected domino product-artemisinin hybrid molecules **11**, **12a**, **12b**, **13a** and **13b**. To our delight, biological tests against HCMV revealed five domino products, **7b**, **12a**, **12b**, **13a** and **13b**, as highly active compounds (EC_{50} values 0.071–1.8 μ M), outperforming the clinical reference drug ganciclovir (EC_{50} 2.6 μ M). In this respect it was found that artemisinin-derived azabicycle **12a** was the most active compound. With respect to the activity against the parasite *P. falciparum* 3D7, three domino products **11**, **13a** and **13b** (EC_{50} values 0.72–1.8 nM) were more potent than the clinically used drug chloroquine (EC_{50} 9.1 nM). Among these three hits, the artemisinin-derived iminocarbocyclic compound **13b** was the most efficient against the *P. falciparum* 3D7 strain. These results are another excellent proof of the hybridization concept and confirm that the multi-step domino reactions are convenient, sustainable, efficient, and direct routes to novel lead structures for medicinal chemistry.

Experimental Section

Chemistry

For details of the 1H and ^{13}C NMR spectroscopy of compounds in this manuscript and their spectra, see the Supporting Information. Complete characterization of the following domino products has been reported previously: *anti*-**2a**, *syn*-**2a**, **2b**, *anti*-**7a**, **7b**, **12a**, **12b**, **13a** and **13b**.^[10]

General Procedure for the Metal-free Multi-Step Domino Reaction

Imidazole (2.5 mg, 0.036 mmol) was added to a stirred solution of the corresponding aldehyde (0.48 mmol) and malononitrile (24 mg, 0.72 mmol) in toluene (1 mL). The reaction mixture was stirred at room temperature for 48 h. The solvent was removed under reduced pressure and the crude product was purified by silica gel column chromatography (hexane/EtOAc, 5:1 to 3:1).

5-Amino-3-(dicyanomethylene)-7-ethyl-8-propyl-2-azabicyclo[2.2.2]oct-5-ene-4,6-dicarbonitrile (*anti*-**3a**)

White solid; 1H NMR (400 MHz, CD_3OD): δ = 4.35 (d, J = 1.9 Hz, 1H), 1.95–1.85 (m, 1H), 1.85–1.79 (m, 1H), 1.65 (dtd, J = 10.3, 4.2, 2.0 Hz, 1H), 1.56–1.33 (m, 3H), 1.25–1.12 (m, 2H), 1.00 ppm (m, 6H); ^{13}C NMR (100 MHz, CD_3OD): δ = 163.9, 154.9, 116.8, 115.6, 114.0, 76.3, 54.0, 53.0, 50.1, 47.9, 36.4, 28.0, 21.0, 14.4, 11.7 ppm; IR (ATR, solid): $\tilde{\nu}$ = 3450, 3323, 3267, 3199, 2966, 2207, 1659, 1607, 1564, 1460, 1408, 1331, 1284, 1225, 1112, 995, 730, 591, 542 cm^{-1} ; MS [MALDI, sinapinic acid (sin), 2,5-dihydroxybenzoic acid (dhb)]: m/z : 307 [$M+H$]⁺, 329 [$M+Na$]⁺; HRMS (ESI): m/z : calcd for $C_{17}H_{18}N_6Na$: 329.1485 [$M+Na$]⁺; found: 329.1487.

5-Amino-3-(dicyanomethylene)-7-ethyl-8-propyl-2-azabicyclo[2.2.2]oct-5-ene-4,6-dicarbonitrile (*syn*-**3a**)

White solid; 1H NMR (400 MHz, $(CD_3)_2CO$): δ = 9.38 (s, 1H), 6.61 (s, 2H), 4.65 (d, J = 1.6 Hz, 1H), 2.54 (td, J = 9.8, 2.0 Hz, 1H), 2.31–2.19 (m, 1H), 1.76–1.45 (m, 5H), 1.34–1.21 (m, 1H), 1.05 (t, J = 7.3 Hz, 3H), 0.99 ppm (t, J = 7.2 Hz, 3H); ^{13}C NMR (100 MHz, $(CD_3)_2CO$): δ = 161.5, 154.9, 115.3, 114.5, 113.9, 112.8, 77.6, 53.4, 52.7, 50.7, 45.2, 45.2, 30.6, 23.3, 21.0, 13.4, 11.7 ppm; IR (ATR, solid): $\tilde{\nu}$ = 3411, 3327, 3204, 2952, 2870, 2206, 1655, 1612, 1574, 1446, 1395, 1319, 1285, 1224, 1201, 1114, 986, 935, 780, 659, 601, 535, 453 cm^{-1} ; MS (MALDI, dhb): m/z : 329 [$M+Na$]⁺; HRMS (ESI): m/z : calcd for $C_{17}H_{18}N_6Na$: 329.1485 [$M+Na$]⁺; found: 329.1477.

6-Amino-8-ethyl-2-imino-7-propylbicyclo[2.2.2]oct-5-ene-1,3,3,5-tetracarbonitrile (**3b**, Mixture of Diastereomers)

White solid; 1H NMR (300 MHz, $(CD_3)_2CO$): δ = 12.58–11.81 (2 \times s, 2 \times 1H), 6.79–6.75 (2 \times s, 2 \times 2H), 3.96–3.90 (1 \times s, 1 \times d, J = 1.8 Hz, 2 \times 1H), 2.00–1.95 (m, 2H), 1.88–1.38 (m, 11H), 1.34–1.17 (m, 3H), 1.09–1.03 (2 \times t, J = 7.4, 7.4 Hz, 2 \times 3H), 1.00–0.94 ppm (2 \times t, J = 7.1, 7.2 Hz, 2 \times 3H); ^{13}C NMR (100 MHz, $(CD_3)_2CO$): δ = 161.7, 160.4, 155.4, 154.2, 116.6, 116.5, 113.8, 113.7, 113.3, 113.1, 112.8, 112.4, 69.4, 68.8, 58.1, 56.3, 46.9, 46.7, 43.8, 43.2, 43.0, 43.0, 42.0, 36.4, 36.3, 28.7, 28.6, 20.7, 20.6, 13.9, 13.8, 11.5, 11.3, 11.3 ppm; IR (ATR, solid): $\tilde{\nu}$ = 3395, 3327, 3238, 2929, 2203, 2157, 1645, 1592, 1458, 1416, 1313, 1244, 1195, 1078, 985, 889, 836, 782, 741, 594, 528,

437 cm⁻¹; MS (MALDI, dhb): *m/z*: 329 [M+Na]⁺; HRMS (ESI): *m/z*: calcd for C₁₇H₁₈N₆Na: 329.1485 [M+Na]⁺; found: 329.1487.

5-Amino-8-butyl-3-(dicyanomethylene)-7-propyl-2-azabicyclo[2.2.2]oct-5-ene-4,6-dicarbonitrile (anti-4a)

White solid; ¹H NMR (400 MHz, (CD₃)₂CO): δ = 9.37 (s, 1H), 6.67 (s, 2H), 4.55 (d, *J* = 1.7 Hz, 1H), 1.99–1.86 (m, 2H), 1.58–1.26 (m, 10H), 0.92 ppm (t, *J* = 6.9 Hz, 6H); ¹³C NMR (100 MHz, (CD₃)₂CO): δ = 162.7, 153.0, 115.4, 112.9, 77.2, 53.1, 52.0, 52.0, 49.2, 48.0, 47.1, 36.3, 33.0, 22.9, 20.1, 13.7, 13.6 ppm; IR (ATR, solid): $\tilde{\nu}$ = 3462, 3423, 3259, 3228, 3182, 2956, 2926, 2859, 2213, 2200, 1655, 1571, 1442, 1396, 1217, 1114, 1058, 985, 867, 638, 590, 544, 448 cm⁻¹; MS [MALDI, om (without matrix)]: *m/z*: 357.2 [M+Na]⁺; HRMS (ESI): *m/z*: calcd for C₁₉H₂₂N₆Na: 357.1798 [M+Na]⁺; found: 357.1792.

5-Amino-8-butyl-3-(dicyanomethylene)-7-propyl-2-azabicyclo[2.2.2]oct-5-ene-4,6-dicarbonitrile (syn-4a)

White solid; ¹H NMR (400 MHz, (CD₃)₂CO): δ = 9.42 (s, 1H), 6.62 (s, 2H), 4.61 (d, *J* = 1.7 Hz, 1H), 2.53 (td, *J* = 10.0, 2.1 Hz, 1H), 2.40–2.29 (m, 1H), 1.85–1.72 (m, 1H), 1.71–1.49 (m, 4H), 1.48–1.24 (m, 5H), 0.94 ppm (2×t, *J* = 6.8 Hz, 6H); ¹³C NMR (75 MHz, (CD₃)₂CO): δ = 161.8, 155.2, 115.7, 114.9, 114.3, 113.2, 78.0, 53.9, 53.8, 51.1, 45.8, 43.8, 32.8, 30.8, 29.0, 23.0, 21.3, 14.3, 14.1 ppm; IR (ATR, solid): $\tilde{\nu}$ = 3418, 3324, 3228, 2957, 2868, 2207, 1657, 1571, 1460, 1400, 1218, 1136, 1061, 977, 938, 872, 648, 597, 536, 455 cm⁻¹; MS (MALDI, dhb): *m/z*: 357.2 [M+Na]⁺; HRMS (ESI): *m/z*: calcd for C₁₉H₂₂N₆Na: 357.1822 [M+Na]⁺; found: 357.1792.

6-Amino-7-butyl-2-imino-8-propylbicyclo[2.2.2]oct-5-ene-1,3,3,5-tetracarbonitrile (4b, Mixture of Diastereomers)

White solid; ¹H NMR (400 MHz, (CD₃)₂CO): δ = 12.58–11.82 (2×s, 2×1H), 6.80–6.75 (2×s, 2×2H), 3.94–3.87 (1×s, 1×d, *J* = 2.2 Hz, 2×1H), 2.17–2.09 (m, 2H), 2.00–1.95 (m, 2H), 1.92–1.73 (m, 2H), 1.60–1.20 (m, 18H), 0.98–0.89 ppm (m, 12H); ¹³C NMR (100 MHz, (CD₃)₂CO): δ = 161.7, 160.5, 155.4, 154.2, 116.6, 116.5, 113.8, 113.7, 113.3, 113.2, 112.9, 112.5, 69.5, 68.8, 58.1, 56.4, 47.0, 46.9, 44.0, 43.2, 43.2, 42.0, 40.8, 37.8, 37.7, 33.9, 33.8, 22.8, 22.8, 20.1, 20.1, 13.5, 13.4 ppm; IR (ATR, solid): $\tilde{\nu}$ = 3402, 3333, 3226, 2960, 2931, 2863, 2200, 1647, 1594, 1461, 1417, 1315, 1245, 1090, 1007, 1055, 1007, 918, 894, 836, 813, 745, 708, 585, 524, 509, 439 cm⁻¹; MS (MALDI, om): *m/z*: 357.2 [M+Na]⁺; HRMS (ESI): *m/z*: calcd for C₁₉H₂₂N₆Na: 357.1798 [M+Na]⁺; found: 357.1808.

5-Amino-7-benzyl-3-(dicyanomethylene)-8-phenethyl-2-azabicyclo[2.2.2]oct-5-ene-4,6-dicarbonitrile (anti-5a)

White solid; ¹H NMR (400 MHz, CD₃CN): δ = 7.42–7.10 (m, 10H), 5.86 (s, 2H), 4.12 (d, *J* = 1.9 Hz, 1H), 2.70 (dd, *J* = 13.9, 6.4 Hz, 1H), 2.62–2.37 (m, 4H), 2.27–2.19 (m, 1H), 2.17–1.96 (m, 2H), 1.49–1.38 ppm (m, 1H); ¹³C NMR (100 MHz, CD₃CN): δ = 163.0, 153.3, 142.5, 139.6, 130.5, 129.8, 129.6, 129.4, 127.9, 127.3, 116.1, 115.1, 115.0, 113.7, 78.6, 54.0, 52.4, 50.6, 49.5, 47.3, 40.2, 35.9, 33.1 ppm; IR (ATR, solid): $\tilde{\nu}$ = 3470, 3369, 3200, 3134, 2924, 2859, 2199, 1644, 1582, 1495, 1447, 1394, 1325, 1277, 1217, 1033, 913, 747, 699, 545, 502 cm⁻¹; MS [MALDI, *trans*-2-[3-(4-*tert*-butylphenyl)-2-methyl-2-prop enylidene]malononitrile (dctb)]: *m/z*: 453 [M+Na]⁺; HRMS (ESI): *m/z*: calcd for C₂₇H₂₂N₆Na: 453.1798 [M+Na]⁺; found: 453.1790; calcd for C₂₇H₂₂N₆K: 469.1538 [M+K]⁺; found: 469.1523.

6-Amino-8-benzyl-2-imino-7-phenethylbicyclo[2.2.2]oct-5-ene-1,3,3,5-tetracarbonitrile (5b, Mixture of Diastereomers)

White solid; ¹H NMR (400 MHz, (CD₃)₂CO): δ = 12.63–11.90 (2×s, 2×1H), 7.52–7.10 (m, 20H), 6.91–6.87 (2×s, 4H), 3.57–3.51 (1×s, 1×d, *J* = 2.1 Hz, 2H), 3.03–2.98 (2×d, *J* = 4.9 Hz, 1H, *J* = 4.9 Hz, 1H), 2.91–2.78 (m, 4H), 2.72–2.66 (m, 2H), 2.63–2.51 (m, 2H), 2.36–2.27 (m, 2H), 2.26–2.15 (m, 1H), 2.14–2.05 (m, 1H), 1.73–1.53 ppm (m, 2H); ¹³C NMR (100 MHz, (CD₃)₂CO): δ = 161.2, 160.2, 155.3, 154.2, 141.2, 141.1, 138.2, 138.2, 129.5, 129.5, 129.3, 129.3, 128.9, 128.9, 128.6, 128.6, 127.4, 127.4, 126.6, 126.6, 116.6, 116.5, 113.6, 113.4, 113.1, 113.0, 112.5, 112.2, 69.3, 68.7, 58.0, 58.0, 56.3, 45.9, 45.9, 44.2, 43.7, 43.6, 43.3, 43.3, 42.0, 41.3, 41.2, 36.3, 33.5, 33.4 ppm; IR (ATR, solid): $\tilde{\nu}$ = 3433, 3343, 3220, 2922, 2856, 2201, 1644, 1598, 1495, 1453, 1412, 1233, 1121, 1056, 1030, 890, 841, 800, 748, 700, 570, 529, 470, 439 cm⁻¹; MS (MALDI, om): *m/z*: 453 [M+Na]⁺; HRMS (ESI): *m/z*: calcd for C₂₇H₂₂N₆Na: 453.1798 [M+Na]⁺; found: 453.1798.

4-Amino-2,6-dimethylcyclohex-4-ene-1,1,3,3,5-pentacarbonitrile (6, Mixture of Diastereomers)

The reaction was performed according to the general procedure for the metal-free multi-step domino reaction with acetaldehyde and malononitrile as starting compounds. The reaction was stirred at room temperature for 24 h. The crude product was purified by column chromatography (pure CH₂Cl₂) to afford **6** as a white solid. M.p. 105 °C; ¹H NMR (400 MHz, (CD₃)₂CO): δ = 7.04–6.97 (s, 2×2H), 3.62 (2×q, *J* = 6.8 Hz, 2×1H), 3.41 (2×q, *J* = 7.0 Hz, 2×1H), 1.88 (d, *J* = 6.8 Hz, 3H), 1.83 (d, *J* = 6.8 Hz, 3H), 1.60 (d, *J* = 6.9 Hz, 3H), 1.55 ppm (d, *J* = 7.0 Hz, 4H); ¹³C NMR (100 MHz, (CD₃)₂CO): δ = 144.5, 143.3, 116.2, 115.6, 113.2, 112.6, 112.3, 112.3, 110.3, 109.9, 109.8, 79.3, 79.3, 42.9, 40.5, 39.8, 39.7, 39.4, 36.4, 36.3, 35.5, 17.3, 17.2, 15.4, 15.1 ppm; IR (ATR, solid): $\tilde{\nu}$ = 3432, 3350, 3230, 2981, 2943, 2884, 2207, 2159, 1648, 1617, 1458, 1372, 1311, 1226, 1155, 1099, 998, 946, 816, 731, 674, 419 cm⁻¹; MS (MALDI, dctb): *m/z*: 273.1 [M+Na]⁺; HRMS (ESI): *m/z*: calcd for C₁₃H₁₀N₆Na: 273.0859 [M+Na]⁺; found: 273.0856.

Reduction with Sodium Borohydride: 2,6-Diamino-7-benzyl-8-phenylbicyclo[2.2.2]octa-2,5-diene-1,3,5-tricarbonitrile (8)

Carbocycle **7b** (29 mg, 0.072 mmol, 1 equiv) was dissolved in methanol (0.6 mL) and cooled to 0 °C. Sodium borohydride (27 mg, 0.72 mmol, 10 equiv) was added and the reaction mixture was stirred for 30 min, before it was allowed to warm to room temperature. After 5.5 h the reaction was quenched by the addition of saturated NaHCO₃ (1 mL). The organic layer was separated and the aqueous phase was extracted with CH₂Cl₂ (3×5 mL). The combined organic phases were washed with brine (15 mL) and dried over Na₂SO₄. The solvent was removed under reduced pressure and the crude product was purified by column chromatography (hexane/EtOAc, 4:1 to 2:1) to give **8** as a white solid (15 mg, 0.040 mmol, 56%). M.p. decomposition > 300 °C; ¹H NMR (400 MHz, (CD₃)₂CO): δ = 7.19–7.10 (m, 2H), 7.11–6.92 (m, 6H), 6.92–6.82 (m, 2H), 6.40–3.40 (2×s, 4H), 3.40 (dd, *J* = 13.0, 3.7 Hz, 1H), 3.19 (d, *J* = 2.5 Hz, 1H), 3.08 (dd, *J* = 4.8, 2.5 Hz, 1H), 3.04–2.97 (m, 1H), 2.52 ppm (dd, *J* = 13.0, 11.6 Hz, 1H); ¹³C NMR (100 MHz, (CD₃)₂CO): δ = 156.9, (156.8), 154.7, (154.6), 142.2, 137.9, 129.7, 128.6, 128.4, 128.0, 126.8, 117.1, 116.8, 114.8, 80.5, (80.4), 78.4, (78.4), 54.3, (54.2), 53.5, 51.6, 45.4, 40.0 ppm; IR (ATR, solid): $\tilde{\nu}$ = 3458, 3395, 3332, 3221, 2917, 2848, 2197, 1658, 1615, 1495, 1454, 1224, 1185, 1161, 1080, 1032, 974, 737, 696, 650, 581, 552, 506 cm⁻¹; HRMS (ESI): *m/z*: calcd for C₂₄H₁₉N₃Na: 400.1533 [M+Na]⁺; found: 400.1539.

4-Amino-2-(dicyanomethyl)pyridine-3,5-dicarbonitrile (9)

Neat domino product **7a** was heated at 150 °C for 17 h. Then, the resulting material was suspended in CH₂Cl₂. After centrifugation (3 min), the precipitate and supernatant were separated. This procedure was repeated twice. The precipitate was dried under high vacuum to afford the pyridine derivative **9** in satisfactory purity as a beige solid (15 mg, 0.072 mmol, 79%). M.p. decomposition > 250 °C; ¹H NMR (400 MHz, (CD₃)₂SO): δ = 8.27 (s, 2H), 8.23 ppm (s, 1H); ¹³C NMR (100 MHz, (CD₃)₂SO): δ = 157.9, 155.0, 149.4, 117.3, 116.2, 113.8, 113.1, 86.7, 78.0, 42.3 ppm; IR (ATR, solid): $\tilde{\nu}$ = 3317, 3207, 3076, 2207, 1655, 1623, 1570, 1510, 1404, 1316, 1259, 1224, 1081, 877, 781, 748, 684, 664, 581, 553, 458, 422 cm⁻¹; HRMS (ESI, negative): *m/z*: calcd for C₁₀H₃N₆: 207.0425 [M-H]⁻; found: 207.0426.

Removal of the solvent of the supernatant under reduced pressure afforded the byproduct (*E*)-prop-1-ene-1,3-diyldibenzene (**10**)^[20] as a colorless oil (6.0 mg, 0.031 mmol, 33%); ¹H NMR (400 MHz, CDCl₃): δ = 7.37–7.26 (m, 7H), 7.23–7.15 (m, 3H), 6.45 (d, *J* = 15.8 Hz, 1H), 6.39–6.25 (m, 1H), 3.54 ppm (d, *J* = 6.6 Hz, 2H); ¹³C NMR (100 MHz, CDCl₃): δ = 140.2, 137.5, 131.1, 129.3, 128.7, 128.6, 128.5, 127.2, 126.2, 126.2, 39.3 ppm; HRMS (APPI): *m/z*: calcd for C₁₅H₁₄: 194.1090 [M]⁺; found: 194.1096.

Domino Isoquinuclidine–Artesunate Hybrid (11)

Artesunic acid (28 mg, 0.073 mmol, 1 equiv) and isoquinuclidine **7a** (29 mg, 0.073 mmol, 1 equiv.) were dissolved in acetonitrile (2.8 mL) under inert conditions (in a nitrogen atmosphere). This solution was cooled to 0 °C, then, DMAP (4.5 mg, 0.037 mmol, 0.5 equiv.) and DCC (20 mg, 0.095 mmol, 1.3 equiv.) were added sequentially. The reaction mixture was stirred for 48 h at 0 °C. The mixture containing a precipitate was filtered and the filtrate was concentrated under reduced pressure. The crude product was purified by column chromatography (hexane/EtOAc, 6:1 to 3:1) to afford **11** as a white solid (22 mg, 0.029 mmol, 39%). M.p. decomposition > 190 °C; ¹H NMR (300 MHz, (CD₃)₂CO): δ = 9.90 (s, 1H), 9.89 (s, 1H), 9.23 (s, 2×1H), 7.18–6.95 (m, 2×10H), 5.73 (d, *J* = 9.8 Hz, 1H), 5.69 (d, *J* = 9.9 Hz, 1H), 5.47 (s, 2×1H), 4.67 (d, *J* = 1.0 Hz, 2×1H), 3.63–3.52 (m, 2×1H), 3.46 (ddd, *J* = 11.3, 7.6, 3.6 Hz, 2×1H), 3.35–3.25 (m, 2×1H), 3.05–2.73 (m, 2×3H), 2.55–2.17 (m, 2×3H), 1.99–1.37 (m, 2×8H), 1.29 (s, 3H), 1.28 (s, 3H), 1.25–0.97 (m, 2×3H), 0.93 (d, *J* = 6.3 Hz, 3H), 0.92 (d, *J* = 6.3 Hz, 3H), 0.85 (d, *J* = 7.1 Hz, 3H), 0.84 ppm (d, *J* = 7.0 Hz, 3H); ¹³C NMR (100 MHz, (CD₃)₂CO): δ = 172.9, 171.1, 170.2, 169.7, 162.7, 162.4, 152.4, 152.3, 140.2, 139.3, 137.0, 136.9, 129.8, 129.7, 129.2, 128.9, 128.6, 128.6, 128.5, 128.2, 128.0, 127.4, 127.2, 126.9, 125.3, 120.3, 115.2, 112.8, 112.5, 112.5, 109.3, 108.6, 104.2, 104.1, 93.0, 92.5, 91.6, 91.5, 80.3, 80.2, 77.9, 77.8, 57.8, 57.1, 53.6, 52.7, 52.3, 52.3, 52.0, 50.8, 50.7, 50.1, 49.2, 48.3, 45.6, 45.6, 39.3, 39.0, 37.1, 37.1, 36.4, 34.6, 34.4, 32.2, 32.1, 30.9, 26.6, 25.5, 24.9, 22.8, 21.8, 21.8, 20.0, 13.8, 11.9, 11.8 ppm; IR (ATR, solid): $\tilde{\nu}$ = 3449, 3347, 3206, 3134, 2926, 2873, 2202, 1720, 1647, 1570, 1495, 1451, 1405, 1379, 1221, 1179, 1158, 1099, 1013, 945, 875, 825, 752, 694, 647, 564, 539, 511 cm⁻¹; HRMS (ESI): *m/z*: calcd for C₄₄H₄₄N₆NaO₇: 791.3164 [M+Na]⁺; found: 791.3163; elemental analysis calcd (%) for C₄₄H₄₆N₆O₈ (M+H₂O): C 67.16, H 5.89, N 10.68; found: C 66.97, H 5.68, N 10.50.

HCMV GFP-Based Replication Assay

An HCMV GFP-based replication assay was performed over a duration of seven days (multi-round infection) using primary human foreskin fibroblasts (HFFs) infected with a GFP-expressing recombi-

nant human cytomegalovirus (HCMV AD169-GFP) as described previously.^[18a,19b] All data represent mean values of determinations in quadruplicate [HCMV infections performed in duplicate, GFP measurements of total cell lysates performed in duplicate using automated quantitative GFP fluorometry in a Victor 1420 Multilabel Counter (PerkinElmer Wallac GmbH, Freiburg, Germany), as described].^[21] Processing and evaluation of data was performed by the use of Excel (means and standard deviations).

Cytotoxicity Studies against *P. falciparum* 3D7 Strains

P. falciparum Culture

P. falciparum 3D7 parasites were cultured in type-A-positive human erythrocytes at a hematocrit of 5% in RPMI 1640 supplemented with HEPES (25 mM), hypoxanthine (0.1 mM), gentamycin (50 µg mL⁻¹) and 0.5% albumax I. Cultures were incubated at 37 °C under controlled atmospheric conditions of 5% O₂, 3% CO₂, and 92% N₂ at 95% relative humidity.

In Vitro Antimalarial Activity Assay

Cultures used in cell proliferation assays were synchronized by treatment with sorbitol.^[22] Effective concentrations to inhibit parasite growth by 50% (EC₅₀) were determined using the SYBR Green I malaria drug-sensitivity assay.^[23] Aliquots (50 µL) of a cell suspension containing ring stages at a parasitemia of 0.2% and a hematocrit of 2% were added to the wells of 96-well microtiter plates. Plates were incubated for 72 h in the presence of drugs at various concentrations. Subsequently, cells of each well were lysed with 2× lysis buffer [Tris (40 mM, pH 7.5), EDTA (10 mM), 0.02% saponin, 0.08% Triton X-100; 50 µL] containing SYBR green (8.3 µM). Plates were incubated for 1 h in the dark at room temperature with constant mixing before the fluorescence (excitation wavelength 485 nm; emission wavelength > 520 nm) was measured using a microtiter plate fluorescence reader (Victor X4, PerkinElmer). Drugs were serially diluted (1:3), with initial drug concentrations of 243 nM for chloroquine and 81 nM for dihydroartemisinin and its derivatives. Each drug concentration was tested in triplicate and repeated at least three times. Uninfected erythrocytes (hematocrit 2%) and infected erythrocytes without drug served as controls and were investigated in parallel. Percent growth was calculated as described by Beez and co-workers.^[24] Data were analyzed using the SigmaPlot (version 12.0; Hill function, three parameters) and SigmaStat (version 13.0) programs.

Acknowledgements

S.B.T. and A.G. gratefully acknowledge financial support from the Deutsche Forschungsgemeinschaft (DFG) by grants TS 87/17-1 and GO 523/16-1 (SPP 1807, Priority Programme “Control of London Dispersion Interactions in Molecular Chemistry”). S.B.T. is also grateful for funding from the DFG (grants TS 87/15-1 and TS 87/16-3) and the Wilhelm Sander-Stiftung (grant 2014.019.1). M.M. and C.H. thank the financial support of the DFG (grant MM 1289/7-3), the Wilhelm Sander-Stiftung (grant 2011.085.2) and the Bayerische Forschungsförderung (ForBIMed-Biomarker in der Infektionsmedizin, grant I1). We also thank the Graduate School Molecular Science (GSMS), Interdisciplinary Center for Molecular Materials (ICMM) and Emerging Fields Initiative (EFI) “Chemistry in Live Cells” supported by Friedrich-Alexander-Universität Erlan-

gen-Nürnberg for research funding and the Elite Network of Bavaria for a doctoral research fellowship for C.M.B.

Conflict of Interest

The authors declare no conflict of interest.

Keywords: antimalarial agents · antiviral agents · density functional calculations · domino reactions · organocatalysis

- [1] a) L. F. Tietze, *Chem. Rev.* **1996**, *96*, 115–136; b) H.-C. Guo, J.-A. Ma, *Angew. Chem. Int. Ed.* **2006**, *45*, 354–366; *Angew. Chem.* **2006**, *118*, 362–375; c) L. F. Tietze, G. Brasche, K. M. Gericke, *Domino Reactions in Organic Synthesis*, Wiley-VCH, Weinheim, **2006**; d) H. Pellissier, *Tetrahedron* **2006**, *62*, 1619–1665; e) H. Pellissier, *Tetrahedron* **2006**, *62*, 2143–2173; f) K. C. Nicolaou, D. J. Edmonds, P. G. Bulger, *Angew. Chem. Int. Ed.* **2006**, *45*, 7134–7186; *Angew. Chem.* **2006**, *118*, 7292–7344; g) C. J. Chapman, C. G. Frost, *Synthesis* **2007**, 1–21; h) D. Enders, C. Grondal, M. R. M. Hüttl, *Angew. Chem. Int. Ed.* **2007**, *46*, 1570–1581; *Angew. Chem.* **2007**, *119*, 1590–1601; i) C. Vaxelaire, P. Winter, M. Christmann, *Angew. Chem. Int. Ed.* **2011**, *50*, 3605–3607; *Angew. Chem.* **2011**, *123*, 3685–3687; j) Ł. Albrecht, H. Jiang, K. A. Jørgensen, *Angew. Chem. Int. Ed.* **2011**, *50*, 8492–8509; *Angew. Chem.* **2011**, *123*, 8642–8660; k) L. F. Tietze, *Domino Reactions: Concepts for Efficient Organic Synthesis*, Wiley-VCH, Weinheim, **2014**; l) C. M. R. Volla, I. Atodiresei, M. Rueping, *Chem. Rev.* **2014**, *114*, 2390–2431.
- [2] a) D. Enders, M. R. M. Hüttl, C. Grondal, G. Raabe, *Nature* **2006**, *441*, 861–863; b) L. Zu, H. Li, H. Xie, J. Wang, W. Jiang, Y. Tang, W. Wang, *Angew. Chem. Int. Ed.* **2007**, *46*, 3732–3734; *Angew. Chem.* **2007**, *119*, 3806–3808; c) Ł. Albrecht, B. Richter, C. Vila, H. Krawczyk, K. A. Jørgensen, *Chem. Eur. J.* **2009**, *15*, 3093–3102; d) K. Jiang, Z.-J. Jia, X. Yin, L. Wu, Y.-C. Chen, *Org. Lett.* **2010**, *12*, 2766–2769; e) D. B. Ramachary, C. Venkaiah, P. Murali, Krishna, *Chem. Commun.* **2012**, *48*, 2252–2254.
- [3] a) Y. Hayashi, T. Okano, S. Aratake, D. Hazeldard, *Angew. Chem. Int. Ed.* **2007**, *46*, 4922–4925; *Angew. Chem.* **2007**, *119*, 5010–5013; b) E. Reyes, H. Jiang, A. Milelli, P. Elsner, R. G. Hazell, K. A. Jørgensen, *Angew. Chem. Int. Ed.* **2007**, *46*, 9202–9205; *Angew. Chem.* **2007**, *119*, 9362–9365.
- [4] a) W.-B. Chen, Z.-J. Wu, Q.-L. Pei, L.-F. Cun, X.-M. Zhang, W.-C. Yuan, *Org. Lett.* **2010**, *12*, 3132–3135; b) W. Sun, G. Zhu, C. Wu, L. Hong, R. Wang, *Chem. Eur. J.* **2012**, *18*, 6737–6741.
- [5] a) O. Mahé, I. Dez, V. Levacher, J.-F. Brière, *Angew. Chem. Int. Ed.* **2010**, *49*, 7072–7075; *Angew. Chem.* **2010**, *122*, 7226–7229; b) C. Yu, Y. Zhang, A. Song, Y. Ji, W. Wang, *Chem. Eur. J.* **2011**, *17*, 770–774.
- [6] a) W. Seebacher, C. Schlapper, R. Brun, M. Kaiser, R. Saf, R. Weis, *Eur. J. Pharm. Sci.* **2005**, *24*, 281–289; b) W. Seebacher, C. Schlapper, R. Brun, M. Kaiser, R. Saf, R. Weis, *Eur. J. Med. Chem.* **2006**, *41*, 970–977; c) M. O. Faruk Khan, M. S. Levi, B. L. Tekwani, N. H. Wilson, R. F. Borne, *Bioorg. Med. Chem.* **2007**, *15*, 3919–3925; d) T. S. Banerjee, S. Paul, S. Sinha, S. Das, *Bioorg. Med. Chem.* **2014**, *22*, 6062–6070.
- [7] a) M. Rueping, C. Azap, *Angew. Chem. Int. Ed.* **2006**, *45*, 7832–7835; *Angew. Chem.* **2006**, *118*, 7996–7999; b) H. Yang, R. G. Carter, *J. Org. Chem.* **2009**, *74*, 5151–5156; c) H. Yang, R. G. Carter, *Tetrahedron* **2010**, *66*, 4854–4859; d) N. Holub, H. Jiang, M. W. Paixão, C. Tiberi, K. A. Jørgensen, *Chem. Eur. J.* **2010**, *16*, 4337–4346; e) D. Wu, Y. H. He, X. Deng, Z. Guan, *J. Heterocycl. Chem.* **2013**, *50*, 425–429; f) A. Alizadeh, V. Sadeghi, F. Bayat, L.-G. Zhu, *Synlett* **2014**, *25*, 2609–2612.
- [8] a) D. Schinzer, M. Kalesse, *Tetrahedron Lett.* **1991**, *32*, 4691–4694; b) Y.-S. Lin, S.-Y. Chang, M.-S. Yang, C. P. Rao, R. K. Peddinti, Y.-F. Tsai, C.-C. Liao, *J. Org. Chem.* **2004**, *69*, 447–458; c) V. Thornqvist, S. Manner, M. Wingstrand, T. Frejd, *J. Org. Chem.* **2005**, *70*, 8609–8612; d) J. Carreras, A. Avenoza, J. H. Busto, J. M. Peregrina, *J. Org. Chem.* **2007**, *72*, 3112–3115; e) H. Nakano, K. Osone, M. Takeshita, E. Kwon, C. Seki, H. Matsuyama, N. Takano, Y. Kohari, *Chem. Commun.* **2010**, *46*, 4827–4829; f) J.-A. Funel, G. Schmidt, S. Abele, *Org. Process Res. Dev.* **2011**, *15*, 1420–1427; g) I. Wauters, A. De Blicq, K. Muylaert, T. S. A. Heugebaert, C. V. Stevens, *Eur. J. Org. Chem.* **2014**, 1296–1304.
- [9] a) M. Igarashi, Y. Nakano, K. Takezawa, T. Watanabe, S. Sato, *Synthesis* **1987**, 68–70; b) Y. Nakano, W.-Y. Shi, Y. Nishii, M. Igarashi, *J. Heterocycl. Chem.* **1999**, *36*, 33–40; c) Y. Nakano, Y. Kaneko, W. A. Fen, *Heterocycles* **1999**, *51*, 169–177; d) N. Mahajan, V. Gupta, P. Kotwal, A. S. Pannu, T. K. Razdan, *J. Chem. Crystallogr.* **2011**, *41*, 552–556.
- [10] C. M. Bock, G. Parameshwarappa, S. Bönisch, C. Neiss, W. Bauer, F. Hampel, A. Görling, S. B. Tsogoeva, *Chem. Eur. J.* **2016**, *22*, 5189–5197.
- [11] a) I. Iriepa, F. J. Villasante, E. Gálvez, L. Labeaga, A. Innerarity, A. Orjales, *Bioorg. Med. Chem. Lett.* **2002**, *12*, 189–192; b) M. E. Kuehne, L. He, P. A. Jokiel, C. J. Pace, M. W. Fleck, I. M. Maisonneuve, S. D. Glick, J. M. Bidlack, *J. Med. Chem.* **2003**, *46*, 2716–2730; c) L. S. Aitken, N. R. Arezki, A. Dell’Isola, A. J. A. Cobb, *Synthesis* **2013**, *45*, 2627–2648; d) E. Cifuentes-Pagano, J. Saha, G. Csanyi, I. Al Ghoulah, S. Sahoo, A. Rodriguez, P. Wipf, P. J. Pagano, E. M. Skoda, *MedChemComm* **2013**, *4*, 1085–1092; e) Y. Watanabe, S. Kitazawa, H. Fujii, T. Nemoto, S. Hirayama, T. Iwai, H. Gouda, S. Hirono, H. Nagasea, *Bioorg. Med. Chem. Lett.* **2014**, *24*, 4980–4983.
- [12] M. R. S. Weir, J. B. Hyne, *Can. J. Chem.* **1965**, *43*, 772–782.
- [13] CSEARCH/NMRPredict software package, W. Robien, University of Vienna, Austria; <http://nmrpredict.orc.univie.ac.at/> last accessed October 24, 2015.
- [14] M. Hoshino, H. Katou, K.-i. Yamaguchi, Y. Goto, *Biochim. Biophys. Acta Biomembranes* **2007**, *1768*, 1886–1899.
- [15] a) L. F. Tietze, H. P. Bell, S. Chandrasekhar, *Angew. Chem. Int. Ed.* **2003**, *42*, 3996–4028; *Angew. Chem.* **2003**, *115*, 4128–4160; b) G. Mehta, V. Singh, *Chem. Soc. Rev.* **2002**, *31*, 324–334; c) A. Ganesan, *Curr. Opin. Biotechnol.* **2004**, *15*, 584–590; d) B. Meunier, *Acc. Chem. Res.* **2008**, *41*, 69–77.
- [16] a) S. B. Tsogoeva, *Mini-Rev. Med. Chem.* **2010**, *10*, 773–793; b) T. Fröhlich, A. Çapçı Karagöz, C. Reiter, S. B. Tsogoeva, *J. Med. Chem.* **2016**, *59*, 7360–7388.
- [17] a) C. Horwedel, S. B. Tsogoeva, S. Wei, T. Efferth, *J. Med. Chem.* **2010**, *53*, 4842–4848; b) C. Reiter, A. Herrmann, A. Çapçı, T. Efferth, S. B. Tsogoeva, *Bioorg. Med. Chem.* **2012**, *20*, 5637–5641; c) C. Reiter, A. Çapçı Karagöz, T. Fröhlich, V. Klein, M. Zeino, K. Viertel, J. Held, B. Mordmüller, S. Emirdağ Öztürk, H. Anıl, T. Efferth, S. B. Tsogoeva, *Eur. J. Med. Chem.* **2014**, *75*, 403–412; d) C. Reiter, T. Fröhlich, L. Gruber, C. Hutterer, M. Marschall, C. Voigtländer, O. Friedrich, B. Kappes, T. Efferth, S. B. Tsogoeva, *Bioorg. Med. Chem.* **2015**, *23*, 5452–5458; e) C. Reiter, T. Fröhlich, M. Zeino, M. Marschall, H. Bahsi, M. Leidenberger, O. Friedrich, B. Kappes, F. Hampel, T. Efferth, S. B. Tsogoeva, *Eur. J. Med. Chem.* **2015**, *97*, 164–172.
- [18] a) M. Marschall, M. Freitag, S. Weiler, G. Sorg, T. Stamminger, *Antimicrob. Agents Chemother.* **2000**, *44*, 1588–1597; b) M. Marschall, T. Stamminger, A. Urban, S. Wildum, H. Ruebsamen-Schaeff, H. Zimmermann, P. Lischka, *Antimicrob. Agents Chemother.* **2012**, *56*, 1135–1137.
- [19] a) S. J. F. Kaptein, T. Efferth, M. Leis, S. Rechter, S. Auerochs, M. Kalmer, C. A. Bruggeman, C. Vink, T. Stamminger, M. Marschall, *Antiviral Res.* **2006**, *69*, 60–69; b) S. Chou, G. Marousek, S. Auerochs, T. Stamminger, J. Milbradt, M. Marschall, *Antiviral Res.* **2011**, *92*, 364–368.
- [20] E. Alacid, C. Nájera, *Org. Lett.* **2008**, *10*, 5011–5014.
- [21] C. Hutterer, I. Niemann, J. Milbradt, T. Fröhlich, C. Reiter, O. Kadioglu, H. Bahsi, I. Zeitträger, S. Wagner, J. Einsiedel, P. Gmeiner, N. Vogel, S. Wandinger, K. Godl, T. Stamminger, T. Efferth, S. B. Tsogoeva, M. Marschall, *Antiviral Res.* **2015**, *124*, 101–109.
- [22] C. Lambros, J. P. Vanderberg, *J. Parasitol.* **1979**, *65*, 418–420.
- [23] M. Smilkstein, N. Sriwilajaroen, J. X. Kelly, P. Wilairat, M. Riscoe, *Antimicrob. Agents Chemother.* **2004**, *48*, 1803–1806.
- [24] D. Beez, C. P. Sanchez, W. D. Stein, M. Lanzer, *Antimicrob. Agents Chemother.* **2011**, *55*, 50–55.

Received: January 11, 2017

Revised manuscript received: March 1, 2017

Version of record online April 26, 2017